The International Journal of Biochemistry & Cell Biology 64 (2015) 212–219

Contents lists available at ScienceDirect

The International Journal of Biochemistry & Cell Biology

journal homepage: www.elsevier.com/locate/biocel

Short communication

Osteogenic differentiation of human MSCs: Specific occupancy of the mitochondrial DNA by NFATc1 transcription factor

Elisabetta Lambertini[a], Letizia Penolazzi[a], Claudia Morganti[b], Gina Lisignoli[c], Nicoletta Zini[d,e], Marco Angelozzi[a], Massimo Bonora[b], Letizia Ferroni[f], Paolo Pinton[b], Barbara Zavan[f], Roberta Piva[a,*]

[a] Department of Biomedical and Specialty Surgical Sciences, University of Ferrara, Ferrara, Italy
[b] Section of Pathology Oncology, Experimental Biology and Laboratory for Technologies of Advanced Therapies (LTTA), Department of Morphology, Surgery, Experimental Medicine, University of Ferrara, Ferrara, Italy
[c] Laboratorio di Immunoreumatologia e Rigenerazione Tissutale, IOR, Bologna, Italy
[d] CNR – National Research Council of Italy, Institute of Molecular Genetics, Bologna, Italy
[e] Laboratory of Musculoskeletal Cell Biology, Istituto Ortopedico Rizzoli, Bologna, Italy
[f] Department of Biomedical Sciences, University of Padova, Padova, Italy

ARTICLE INFO

Article history:
Received 20 January 2015
Received in revised form 9 April 2015
Accepted 21 April 2015
Available online 5 May 2015

Keywords:
Osteogenic differentiation
Mesenchymal stem cells
Mitochondria
NFATc1
Chromatin immunoprecipitation assay

ABSTRACT

A substantial body of evidence indicates that mitochondrial morphology and function change during osteogenic differentiation. However, molecular mechanisms linking mitochondrial dynamics with the regulation of osteoblast functions are poorly understood. Amongst the molecules that influence the decision of human mesenchymal stem cells (hMSCs) to become osteoblasts are Slug and NFATc1 transcription factors (TFs). These molecules also interfere with different mitochondria-dependent pathways in response to a variety of cellular demands. The present study investigated the recruitment of Slug and NFATc1 at the D-loop regulatory region of mitochondrial DNA (mtDNA) in osteogenic differentiated hMSCs with the aim of exploring whether Slug and NFATc1 also act as mitoTFs in the mitochondrial pool of nuclear TFs.

The results demonstrate that NFATc1, but not Slug, is localized in the mitochondria. Using chromatin immunoprecipitation assay, we found that NFATc1 is recruited at mtDNA, but this occurs only when the calcification process is at its highest in osteo-induced MSC and the maximum level of differentiation is reached. Occupancy of the mtDNA by NFATc1 is associated with a decreased expression of crucial mitochondrial genes such as Cytochrome B and NADH dehydrogenase 1. This suggests that NFATc1 acts as a negative regulator of mtDNA transcription during the calcification process and interruption of aerobic energy demand.

The finding of NFATc1 participation in osteogenic differentiation through its direct involvement in the regulatory machinery of mitochondria suggests a new role for this TF and adds information on communication between mitochondrial and nuclear genomes.

1. Introduction

Variations of number, structure, function and intracellular distribution of mitochondria are correlated with cell functionality and different cell energy demands (Kuznetsov and Margreiter, 2009). These variations, which are strictly associated with a finely tuned crosstalk between the mitochondrial and nuclear genomes, have recently been recognized as essential events during the differentiation process of stem cells and cell fate switch (Parker et al., 2009; Mandal et al., 2011; Folmes et al., 2012; Bukowiecki et al., 2014; Wanet et al., 2014). Efforts to uncover the mechanisms of mitochondrial biogenesis as well as to characterize energy metabolism and redox status during cell differentiation have been made (Chen et al., 2008, 2010; Madeira, 2012), but little is known about mitochondria transcription regulation by lineage-specific factors and signaling demands. In particular, molecular regulatory circuits that govern mitochondrial dynamics together with mitochondrial contribution to differentiation potential of stem cells remain poorly understood.

* Corresponding author at: Department of Biomedical and Specialty Surgical Sciences, University of Ferrara, Via Fossato di Mortara, 74 44121 Ferrara, Italy. Tel.: +39 0532974405; fax: +39 0532974405.
E-mail address: piv@unife.it (R. Piva).

http://dx.doi.org/10.1016/j.biocel.2015.04.011
1357-2725/

Hence, exploring the properties of mitochondria during differentiation of cellular progenitors is important in gaining information on stem cell biology, and developing new pharmacologic strategies in regenerative medicine. In addition this may facilitate the understanding of maintenance of cell culture homeostasis and the optimization of *in vitro* cell differentiation protocols by adjusting some biochemical properties, such as energy production or redox status of mitochondria. These improvements could provide high quality stem cells to be used for cell therapy with mitochondrial properties being used as a quality measure of cell-based products for several clinical use.

Recent studies have shown that mitochondrial DNA copy number, protein subunits of the respiratory enzymes and intracellular ATP content, increased together with the efficiency of oxidative phosphorylation during osteogenic differentiation of adult human mesenchymal stem cells (hMSCs) (Chen et al., 2008; Pietilä et al., 2010). Growing evidence supports the bifunctional role of many transcription factors (TFs) in the control of both nuclear and mitochondrial gene expression (Szczepanek et al., 2012; Leigh-Brown et al., 2010).

Two nuclear TFs, Slug/Snail2 (Cobaleda et al., 2007) and NFATc1 (nuclear factor of activated T cells complex 1) (Horsley and Pavlath, 2002), have been recently described as osteogenic modulators (Lambertini et al., 2009; Deng et al., 2008; Koga et al., 2005; Penolazzi et al., 2011).

Slug belongs to the highly conserved Slug/Snail family of transcription factors with an essential role in development and in many cellular functions including control of stem cell properties (Cobaleda et al., 2007). NFAT proteins comprise a family of transcription factors (NFAT 1-5) that, after calcium/calcineurin-dependent dephosphorylation, are activated and regulate the expression of many genes involved in a wide range of cellular processes (Hogan et al., 2003).

This study aimed to explore if Slug and NFATc1 are possible mitoTFs in the mitochondrial pool of nuclear TFs. Published data indicates that these TFs are associated with mitochondria functions. Slug which interferes with the mitochondria-dependent apoptotic pathway (Wu et al., 2005), may regulate mitochondrial ROS production (Kim et al., 2011), and supports the propagation of the stress signaling transcriptional network organized by CREB and HMGA2 in mitochondrial dysfunction (Shibanuma et al., 2012). NFATc1, through calcineurin and calmodulin, is implicated in the regulation of gene expression by calcium signaling, the control of which involves the mitochondria (Kim and Usachev 2009; Chen et al., 2007; Stern, 2006).

The study also aimed to further characterize mitochondria during differentiation of hMSCs toward osteogenesis, and examine whether osteogenic transcription factors (TFs) are also present in the mitochondria. Whether Slug and NFATc1 can be good candidates in the communication between mitochondrial and nuclear genomes, and can contribute to the behavior of MSCs in differentiating toward osteogenic lineage through the regulation of mitochondrial gene expression was also examined.

2. Materials and methods

2.1. Cell culture and differentiation

Human mesenchymal stem cells (hMSC) were isolated from human adipose tissues of five healthy women and five healthy men (age: 21–36) undergoing cosmetic surgery procedures (University of Padova, Plastic Surgery Clinic). The tissue samples were digested with 0.075% collagenase (type 1A; Sigma–Aldrich Chemical Co., St. Louis, MO) in a modified Krebs–Ringer buffer (KRB) [125 mM NaCl, 5 mM KCl, 1 mM Na_3PO_4, 1 mM $MgSO_4$, 5.5 mM glucose, and 20 mM Hepes (pH 7.4)] for 60 min at 37 °C, followed by 10 min with 0.25% trypsin. Floating adipocytes were discarded, and cells from the stromal-vascular fraction were pelleted, rinsed with media, and centrifuged (Gardin et al., 2011). The resulting viable cells were counted using the trypan blue exclusion assay and seeded at a density of 10^6 cells per cm^2 for *in vitro* expansion, in Dulbecco's modified Eagle's medium low-glucose supplemented with 10% fetal bovine serum (Euroclone S.p.A., Milan, Italy), 2 mM L-glutamine, antibiotics (penicillin 100 μg/mL and streptomycin 10 μg/mL), at 37 °C in a humidified atmosphere of 5% CO_2.

hMSCs were used at passage 3 and characterized by testing a panel of surface markers using flow cytometry as previously described (Torreggiani et al., 2012). hMSC from all samples were positive for CD90, CD73, CD105 (mesenchymal cell markers), but negative for CD34, and CD45 (haematopoietic cell markers) (Supplemental Fig. 1A). Multilineage differentiation potentials in response to specific differentiating agents have been confirmed in all samples analyzed. Alizarin Red staining was used to reveal the ability of the cells to deposit a mineral matrix that is a characteristic of osteoblastic lineage. Alcian Blue staining was used to show sulfated proteoglycan deposits that are indicative of chondrogenic differentiation. Oil Red-O staining was employed to demonstrate the formation of lipid droplets after induction of adipogenic differentiation (see Supplemental Fig. 1B).

hMSCs were cultured up to 28 days in DMEM high glucose (Euroclone S.p.A.) supplemented with 10% FBS, 10 mM β-glycerophosphate, 10^{-7} M dexamethasone and 100 mM ascorbate (Sigma–Aldrich) for osteogenic differentiation. The cells were fixed with 70% ethanol for 1 h and then stained with 40 mM Alizarin Red S solution (pH 4.2) at room temperature for 10 min. Cells were then photographed by an optical Leitz microscope.

2.2. Quantitative real-time RT-PCR

Cells were harvested and total RNA was extracted using an RNeasy Mini Kit (Qiagen, Hilden, Germany) in accordance with the manufacturer's instruction. Quantitative real-time PCR was performed using gene expression master mix (Life Technologies, Carlsbad, CA, USA) and analyzed on CFX96 Real-Time detection System (Bio-Rad laboratories, Hercules, CA, USA). Assays-On-Demand kits (Life Technologies) for human *OC*, *ON*, *OPN*, *Runx2*, *COL1A1*, *ALP*, *BMP2*, *BMP7*, *Slug*, *NFATc1*, *ND1* and *CYTB* were used. The expression level of cDNA samples was normalized to the expression of reference GAPDH using the formula $2^{-\Delta Ct}$ or as fold change using the formula $2^{-\Delta\Delta Ct}$. For each hMSC sample the mean of technical triplicates was calculated, and all data are presented as the mean of values from six samples.

2.3. Immunocytochemistry

hMSC grown in chamber slides were fixed in ice-cold methanol and then permeabilized with 0.2% (v/v) Triton X-100 (Sigma–Aldrich) in TBS (Tris-buffered saline). After blocking with 2% normal horse serum (Vectorlabs, Burlingame, CA, USA), hMSCs were incubated with primary antibody for 16 h at 4 °C. The following primary antibodies were used: rabbit anti-human Col1A1 (H-197, 1:100), rabbit anti-human OPN (LF-123, 1:100) and rabbit anti-human RUNX2 (M-70, 1:100) (Santa Cruz Biotechnology, Dallas, TX, USA). Cells were then rinsed and incubated with ImmPRESS™ (Peroxidase) Polymer Universal Anti-Mouse/Rabbit Ig Reagent (Vectorlabs) for 30 min. After washing, the cells were stained with Vectastain ABC reagent and DAB substrate kit for peroxidase (Vectorlabs), mounted in glycerol/TBS 9:1 and observed using a Leitz microscope.

2.4. Immunofluorescence and confocal analysis

hMSC were stained with 100 nM Mitotracker Orange CMTM-Ros (Life Technologies) for 15 min at 37 °C and fixed in 4% paraformaldehyde/PBS. After three washes with TBS, the cells were permeabilized with 0.2% Triton X-100 and then blocked with TBS 2.5% FCS. Cells were then incubated over night at 4 °C with antibodies (Santa Cruz) against human NFATc1 (clone H-110, 1:20), SLUG (clone H-140, 1:20), TFAM (clone H-203, 1:100). Finally primary antibodies were revealed by means of Alexa Fluor® 488 Goat Anti-Rabbit IgG (H+L) (1:100) (Life Technologies). Images were obtained using a Axiovert 220M microscope equipped with a 100× oil immersion Plan-Neofluar objective (NA 1.3, from Carl Zeiss, Jena, Germany) and a CoolSnap HQ CCD camera. The images were background corrected, and Pearson's coefficient for co-localization was analyzed using the JACOP plugin of the open source Fiji software (http://fiji.sc/Fiji).

2.5. Immunogold labeling and electron microscopy

hMSCs were fixed in 1% glutaraldehyde in 0.1 M phosphate buffer pH 7.4 for 1 h, partially dehydrated up to 70% ethanol and embedded in London Resin White (LR White) at 0 °C. Thin sections were pre-incubated with 5% normal goat serum in 0.05 M Tris–Cl, pH 7.6, 0.14 M NaCl, 0.1% BSA (TBS I), incubated overnight at 4 °C with rabbit anti-human NFATc1 (Santa Cruz, clone H-110, 1:10 dilution in TBS I) and then with a goat anti-rabbit conjugated with 15-nm colloidal gold particles (BBInternational, Cardiff, UK) diluted 1:20 in 0.02 M Tris–HCl, pH 8.2, 0.14 M NaCl and 0.1% BSA for 1 h at room temperature. Thin sections were stained with aqueous uranyl acetate and lead citrate and observed with a Zeiss EM109 transmission electron microscope. Images were captured using a Nikon digital camera Dmx 1200F, and ACT-1 software.

2.6. Subcellular fractionation and Western blot analysis

hMSCs were harvested and gently disrupted by homogenization with a previously used method (Bononi and Pinton, 2015). The homogenate was centrifuged twice at 1000 × *g* for 5 min to remove nuclei and unbroken cells (nuclear fraction) and then the supernatant was centrifuged 10,000 × *g* for 10 min. The resultant supernatant was used for cytosolic fraction isolation, while the pellet, consisting of the mitochondrial fraction, was subjected to 100 μM Proteinase K (Sigma–Aldrich) for 30 min on ice. Proteins from the three subcellular fractions were electrophoresed on 12% SDS-polyacrylamide gel and transferred onto an Immobilon-P PVDF (Millipore, Billerica, MA). After blocking the following primary antibodies were used: VDAC (mouse anti-human, 1:2000, Millipore, Billerica, MA), Lamin B1 (mouse anti-human, 1:1000, Santa Cruz) and NFATc1 (rabbit anti-human, 1:500, Santa Cruz Biotechnology). After washing, the membranes were incubated with HRP-conjugated anti-mouse (1:2000) or anti-rabbit (1:50,000) antibodies (Dako, Glostrup, Denmark) and signals were detected by SuperSignal West Femto Substrate (Pierce, Rockford, IL, USA).

2.7. Chromatin immunoprecipitation (ChIP)

ChIP assay was performed using a ChIP Assay Kit (catalog no. 17-295, Upstate) following the manufacturer's instructions. After crosslinking the chromatin with 1% formaldehyde at 37 °C for 10 min, cells were washed with cold PBS, scraped and collected on ice, lysed and sonicated. An equal amount of chromatin was immunoprecipitated at 4 °C overnight with 5 μg of the following antibodies: TFAM, Slug, NFATc1, or non-specific IgG (Santa Cruz). Immunoprecipitated products were collected after incubation with Protein A-agarose beads. The beads were washed, and the bound chromatin was eluted in ChIP eluition buffer. The samples were incubated at 65 °C overnight to reverse the crosslinking. Then the proteins were digested with Proteinase K for 1 h at 45 °C and DNA was purified in 50 μL of Tris–EDTA with a PCR purification kit (Qiagen) according to the manufacturer's instructions. The DNA precipitates and Input (1% of total chromatin used for the immunoprecipitation) were further subjected to semi-quantitative or quantitative PCR using the following primers for amplification of 286-bp fragment of the D-loop region (D-loop forward, 5′-CCC CTC ACC CACTAGGATAC-3′, and D-loop, reverse, 5′-ACG TGT GGG CTA TTT AGG C-3′). PCR products were analyzed by agarose gel electrophoresis and visualized by UV light apparatus. Real-time PCR analyses of the ChIP samples were carried with CFX96 Real-Time detection System (Bio-Rad labs) using iTaq Universal SYBR Green SuperMix (Bio-Rad). We analyzed ChIP-qPCR data relative to Input signal and presented as fold increase in signal relative to the background signal (IgG).

2.8. Statistical analysis

Student's *t* test was used for comparisons between the groups. $p < 0.05$ was considered significant.

3. Results and discussion

3.1. hMSC osteogenic differentiation and mitochondria

We focused on the ability of hMSCs to differentiate toward osteoblastic lineage in order to add information on the functional link between mitochondria and osteogenic differentiation. As shown in Fig. 1A and B, osteogenic induced cells increased the expression of typical osteogenic markers. These include: the main constituent of the organic part of the bone extracellular matrix (ECM) Collagen type I (Col1A1), alkaline phosphatase (ALP) which is responsible for the ECM mineralization, the master regulator of osteogenic differentiation runt-related transcription factor 2 (Runx2), three non-collagenous ECM proteins, osteopontin, osteonectin and osteocalcin, three osteogenic growth factors (BMP2, BMP7 and WNT3). Moreover, the cells produced Alizarin Red positive nodular aggregates at the end of differentiation (day 28).

The mitochondrial morphology was assessed by Mitotracker Orange staining at an early stage of osteogenic differentiation (day 14) when oxidative demand induced by osteogenic medium is high. As shown in Fig. 1C, relative mitochondrial network area per cell was significantly increased in osteogenic induced cells, while no significant alterations were observed in average particle area or form factor.

There are many open questions regarding the signaling pathways and key molecules supporting mitochondria changes in response to specific cell processes such as osteogenic differentiation. The need to respond to this issue is important both for defining the complexity of human mitochondrial transcription machinery, and for understanding the increasing number of diseases associated with mitochondrial dysfunction. Specifically, this approach may be useful to provide new information toward the development of novel therapeutics for bone disorders and bone tissue regeneration.

3.2. NFATc1, but not Slug, is associated with mitochondria

qRT-PCR analysis confirmed that hMSCs express substantial levels of Slug and NFATc1 transcription factors both at basal condition (day 0) and after osteogenic differentiation. mRNA for Slug significantly increased in osteogenic differentiated hMSCs compared to undifferentiated ones (Fig. 2A).

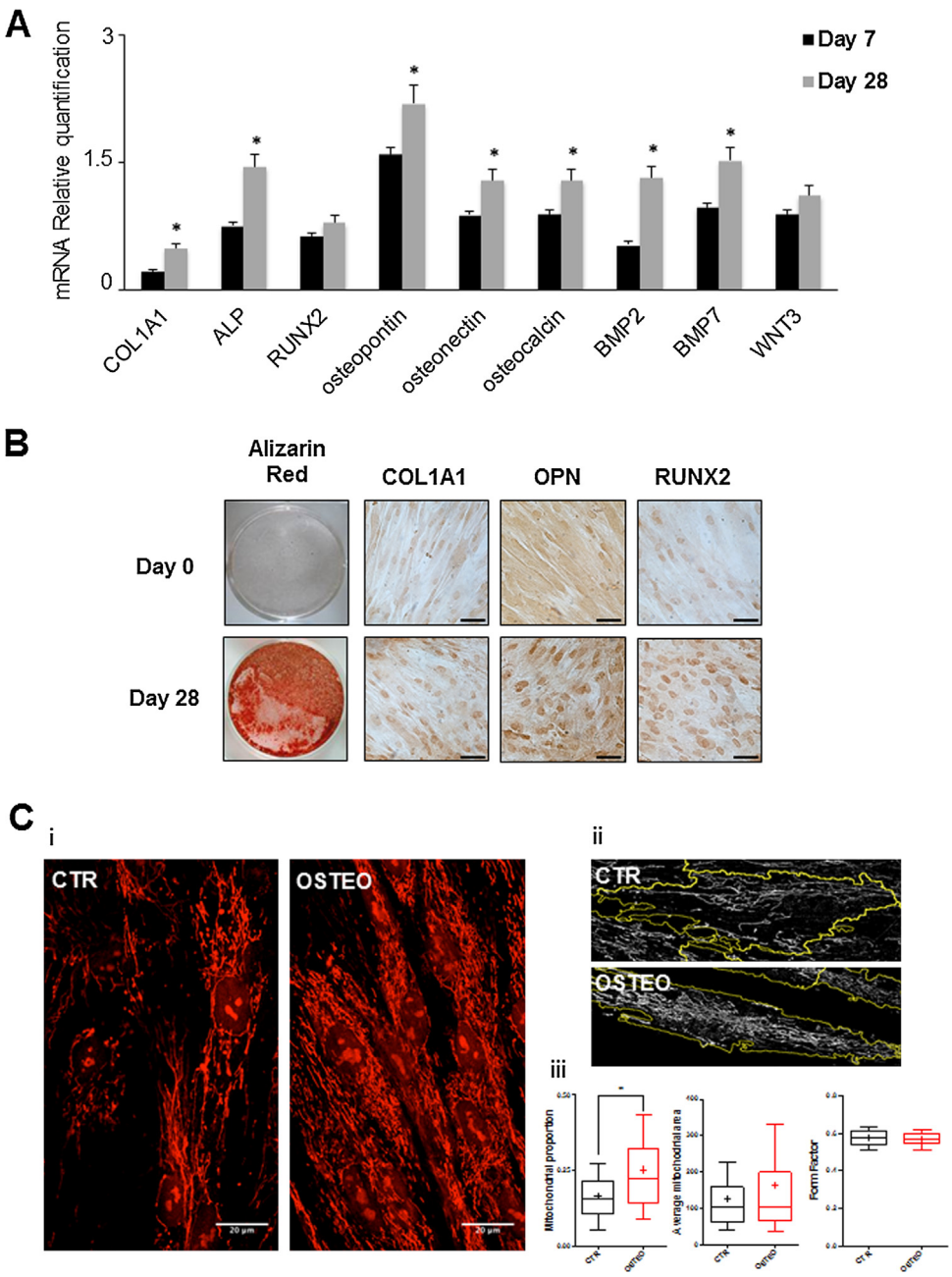

Fig. 1. Osteogenic differentiation of human mesenchymal stem cells (hMSCs) and evaluation of specific markers. (A) Quantitative gene expression analysis of specific osteogenic markers was performed in hMSC induced toward osteogenic differentiation for 28 days. For each cDNA sample, the Ct of the reference gene GAPDH was subtracted from the Ct of the target sequence to obtain the ΔCt. Relative gene expression was then calculated using the $2^{-\Delta Ct}$ method. Error bars represent means ± standard deviation for $n = 6$. *p-value <0.05 compared to day 7 sample group. (B) Mineral matrix deposition was evaluated by ARS staining in hMSCs at day 0 and after 28 days of culture in osteogenic medium. The expression levels of Collagen type 1 (COL1A1), osteopontin (OPN) and RUNX2 were analyzed by immunocytochemistry. Scale bar 50 μm. (C) Morphological aspect of hMSC mitochondria. The amount of mitochondria was evaluated by optical microscopy (i) on hMSC stained with Mitotracker Orange after 14 days of culture in presence (OSTEO) or absence (CTR) of osteogenic inducers. Images were segmented for cell surface and mitochondrial area (see representative sample in ii) to allow quantitation of relative mitochondrial amount, mitochondrial area and morphology (iii). * Significant at $p < 0.05$; line = median, cross = mean, bars = maximum and minimum values. The boxes envelop the 10th to the 90th percentile of the assayed population.

The in-silico analysis performed by two different tools, MitoProt and TargetP, predicts high probability of mitochondrial localization of some NFATc1 isoforms. MitoProt alone predicts a slight probability for Slug to reach mitochondria (Table 1).

NFATc1 and Slug localization were then investigated by immunostaining and confocal microscopy co-localization analysis (Fig. 2B). Interestingly, NFATc1 displays significant co-localization with the mitochondrial marker Mitotracker Orange (as indicated by Pearson's coefficient) to an extent comparable to the transcription factor A mitochondrial (TFAM) which is a crucial activator of mitochondrial transcription and genome duplication. On the contrary Slug remains predominantly localized in the nucleus. Immunogold labeling and Western blot analysis confirmed the association of NFATc1 with the mitochondria (Fig. 2C and D).

Treatment with osteogenic inducers did not affect the localization of these two bone associated transcription factors (data not shown).

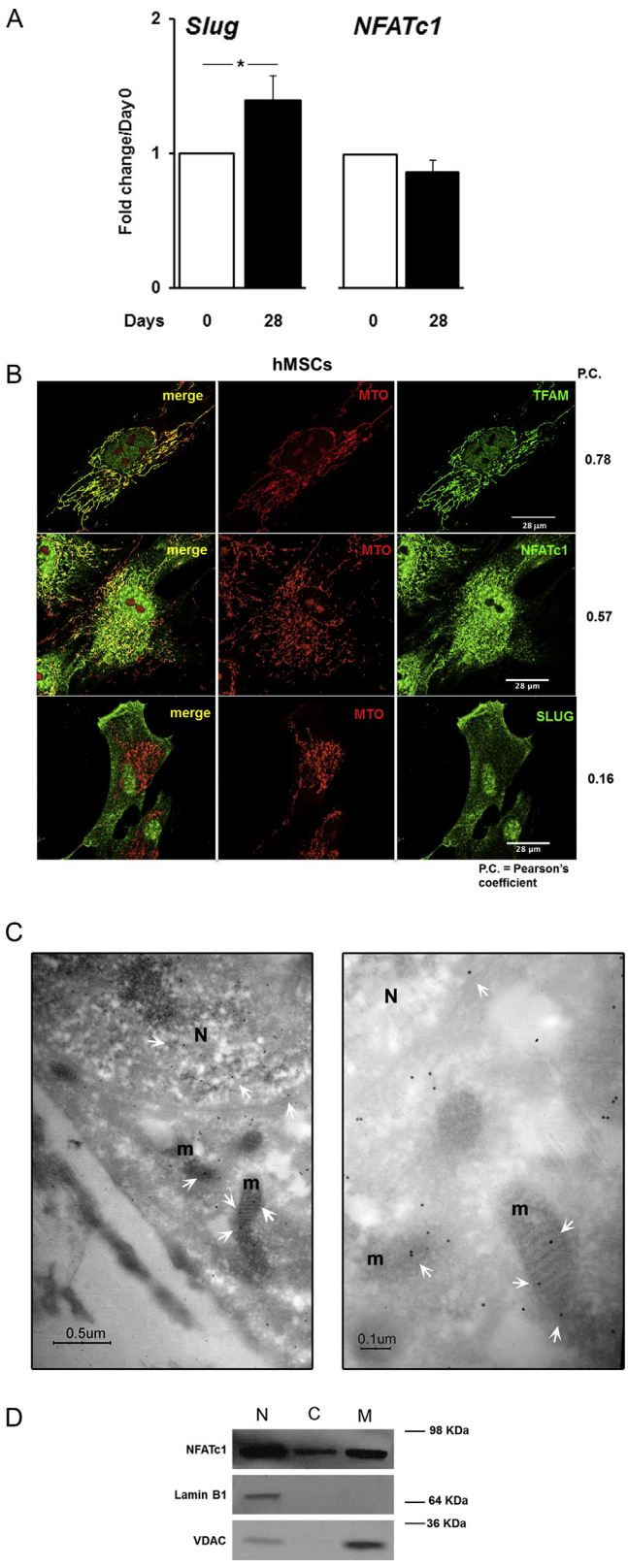

Fig. 2. Mitochondrial localization of NFATc1 and Slug. (A) Slug, and NFATc1 gene expression was determined at mRNA level in hMSCs induced toward osteogenic differentiation for 28 days, and revealed by quantitative RT-PCR. Data were normalized to GAPDH according to the formula $2^{-\Delta\Delta Ct}$ and scaled relative to day 0 expression levels. Results represent means ± S.E.M. of six independent experiments. $^{*}p$-value <0.05 were considered statistically significant. (B) hMSCs were treated with Mitotracker Orange (MTO, red staining) and antibodies (green staining) against TFAM, NFATc1 or Slug. Merge images represent an overlay of the two channels where co-localization is indicated by a color change (yellow). (C) Immunogold labeling of NFATc1 in mitochondria of hMSC cells. Arrows indicate gold particles; m, mitochondria; n, nucleus. (D) Nuclear (N), cytoplasmic (C) and mitochondrial (M) fractions were analyzed by Western blot for NFATc1 expression. Lamin B1 and VDAC1 were used as markers for the purity of the nuclear and mitochondrial fractions, respectively. The data are representative of three independent fractionation experiments. (For interpretation of the references to color in this figure legend, the reader is referred to the web version of this article.)

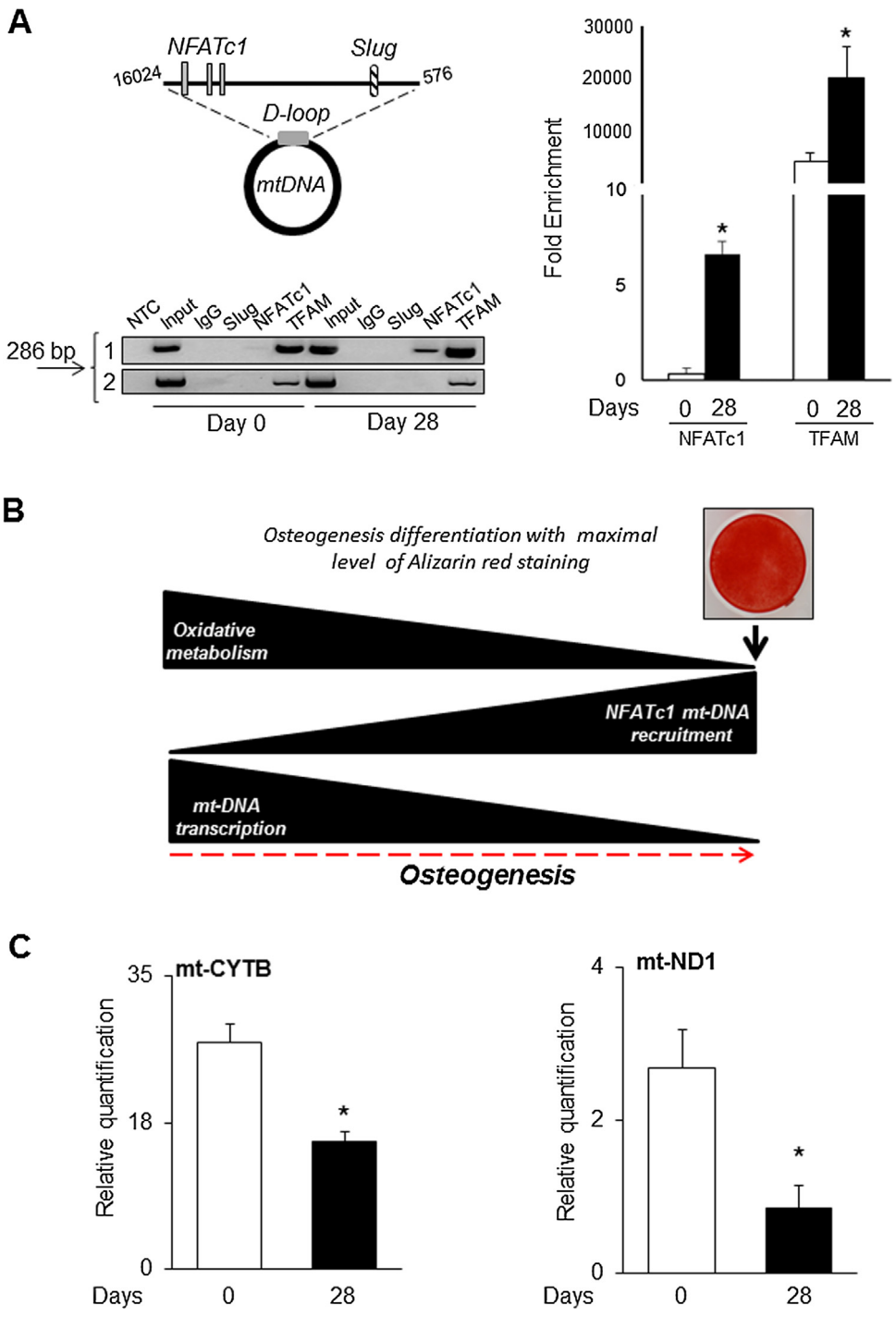

Fig. 3. Recruitment of transcription factors (TFs) at the non-coding region (D-loop) of hMSC mitochondrial DNA. (A) Schematic representation of D-loop region with binding sites for NFAT and Slug TFs is reported. hMSCs at day 0 and after 28 days of culture in osteogenic medium were subjected to chromatin immunoprecipitation (ChIP) assay using antibodies against Slug, NFATc1 and TFAM TFs. A non-specific IgG antibody was used as control. Representative semiquantitative PCRs after ChIP assay are shown. NTC, no template control; Input, positive control; 1, osteogenic differentiated hMSCs sample; 2, hMSCs sample unable to differentiate toward osteogenic lineage. In order to evaluate the fold enrichment relative to the IgG control, quantitative PCR was performed on osteogenic differentiated hMSCs samples. Data represent mean ± S.E.M. ($n = 6$). (B) The hypothesis of relationship between NFATc1 and mitochondrial activity during osteogenic differentiation of hMSCs is schematized. (C) Analysis of mt-DNA transcription in osteogenic differentiated hMSCs. Cells were cultured in presence of osteogenic inducers for 28 days and mRNA expression level of mt-CYTB and mt-ND1 was determined by quantitative RT-PCR. For each cDNA sample, the Ct of the reference gene GAPDH was subtracted from the Ct of the target sequence to obtain the ΔCt. Relative gene expression was then calculated using the $2^{-\Delta Ct}$ method. Data represent mean ± S.E.M. of six independent experiments. *p-value <0.05 compared to day 0 sample group.

3.3. NFATc1 is recruited at mtDNA

A chromatin immunoprecipitation (ChIP) assay was performed to analyze the recruitment of Slug and NFATc1 at the non-coding displacement loop (D-loop) regulatory region of mtDNA (Hock and Kralli, 2009) in order to explore functional regulatory role of Slug and NFATc1 nuclear transcription factors in mitochondria. Mitochondrial genes are densely packed along the genome with the

Table 1
Prediction of mitochondrial localization of the known NFATc1 isoforms and Slug by the informatical tools MitoProt and TargetP.

Target	TargetP	MitoProt	
	Predicted subcellular localization	Probability of export	Cleavage sequence
NFATc1 A-alpha	Mitochondria	0.1448	MPSTSFPVPSKFPLGPAAAVFGRGETLGPAPRA
NFATc1 A-alpha'	–	0.0599	NA
NFATc1 B-alpha	Mitochondria	0.1444	MPSTSFPVPSKFPLGPAAAVFGRGETLGPAPRA
NFATc1 B-beta	–	0.0052	NA
NFATc1 C-alpha	Mitochondria	0.1343	MPSTSFPVPSKFPLGPAAAVFGRGETLGPAPRA
NFATc1 C-beta	–	0.0054	NA
NFATc1 1A-deltaIX	Mitochondria	0.1433	MPSTSFPVPSKFPLGPAAAVFGRGETLGPAPRA
NFATc1 1B-deltaIX	–	0.0053	NA
SNAI2	–	0.5571	NA

exception of D-loop which is devoted to transcription initiation carried out by the mitochondrial-specific RNA polymerase (Shutt et al., 2011; Marinov et al., 2014).

Several reports have suggested that TFs, that typically act in the nucleus, might also have regulatory functions in mitochondrial transcription (Leigh-Brown et al., 2010; Hock and Kralli, 2009; Szczepanek et al., 2012). These include: CREB, NF-kB, ER, MEF2D, STAT1, T3 receptor p43, p53, IRF3, and STAT3. However, direct evidence of protein–DNA contacts in mitochondria has been provided by ChIP analysis only for p53, CREB, and MEFD2 (Leigh-Brown et al., 2010).

The Transcription Element Search Software (TESS) for TF search and MatInspector 7.4 programs identified the presence of one putative Slug binding site (E-box motifs, 5′-CACCTG/CAGGTG-3′) and three NFAT binding sites (5′-GGAAA-3′) in the D-loop region (Fig. 3A).

The ChIP assays results demonstrate that in all the conditions examined Slug is not recruited at appreciable levels. In hMSC samples that fail osteogenic differentiation the D-loop region chromatin was not immunoprecipitated by either Slug or by NFATc1 (see the n.2 representative sample in Fig. 3A). Conversely, the D-loop region is highly occupied by NFATc1 in hMSCs that undergo osteogenesis and this recruitment increased when the cells reach the end of the differentiation process (day 28). TFAM, which is required for initiation and regulation of mitochondrial transcription, was properly recruited by its recognition site at a high level regardless of the presence of differentiating agents. Recent studies demonstrate that mitochondria are maintained at a low activity state in hMSCs. Upon osteogenic induction, their functions increase to fulfill a higher degree of energy demand or to facilitate other biochemical reactions that take place within the organelles. However, the high energy aerobic demand by osteoblasts at the early stages of differentiation, is necessarily slowed down during the progress of calcified matrix deposition and at the end of differentiation when the cells become apoptotic or quiescent. The regulation of these dynamics has still to be studied but it is reasonable to hypothesize that specific signals are sent from the nucleus to mitochondria to change their activities (Cagin and Enriquez, 2015). Our data are consistent with this hypothesis, suggesting that one of these signals could be represented by NFATc1 acting as a negative regulator of mtDNA transcription. NFATc1 could contribute to the calcification process participating in the interruption of aerobic energy demand when it is no longer needed (see the scheme in Fig. 3B).

This hypothesis is also supported by the expression level of crucial mitochondrial genes. As shown in Fig. 3C, a decrease of CytB (Cytochrome B) and ND1 (NADH dehydrogenase 1) expression at the end of the osteogenic differentiation was observed.

Our preliminary evidence regarding NFATc1 in osteogenesis sheds light on the controversial role of NFATc1 in osteoblastic differentiation and function. Recent studies have demonstrated that activation of NFATc1 promotes osteoblast differentiation *in vitro* and *in vivo* (Koga et al., 2005; Fromigue et al., 2010; Ogasawara et al., 2013). Other evidence supports the inhibitory effects of NFATc1 on osteoblast differentiation through different pathways (Yeo et al., 2007; Zanotti et al., 2011) so, the role of NFATc1 in osteoblasts could be different, depending on its interaction with other specific molecules.

Our data on the potential involvement of NFATc1 in mineralization process, are in agreement with recent reports that indicate the implication of this transcription factor in vascular calcification (Goettsch et al., 2011).

The results of this study suggest a new role of NFATc1. Further studies are required for a better understanding of its involvement in the regulatory machinery of mitochondria in relation to osteoblast function and energetic metabolism.

Conflict of interest statement

No conflicts of interest, financial or otherwise, are declared by the authors.

Acknowledgements

The authors thank Dr. Amanda J. Neville for her linguistic support in revising the manuscript. This work was supported by Fondazione Cassa di Risparmio di Padova e Rovigo, Italy.

Appendix A. Supplementary data

Supplementary material related to this article can be found, in the online version, at http://dx.doi.org/10.1016/j.biocel.2015.04.011

References

Bononi A, Pinton P. Study of PTEN subcellular localization. Methods 2015;77:92–103.
Bukowiecki R, Adjaye J, Prigione A. Mitochondrial function in pluripotent stem cells and cellular reprogramming. Gerontology 2014;60:174–82.
Cagin U, Enriquez JA. The complex crosstalk between mitochondria and the nucleus: what goes in between? Int J Biochem Cell Biol 2015;63:10–5.
Chen CT, Hsu SH, Wei YH. Upregulation of mitochondrial function and antioxidant defense in the differentiation of stem cells. Biochim Biophys Acta 2010;1800:257–63.
Chen CT, Shih YR, Kuo TK, Lee OK, Wei YH. Coordinated changes of mitochondrial biogenesis and antioxidant enzymes during osteogenic differentiation of human mesenchymal stem cells. Stem Cells 2008;26:960–8.
Chen Y, Yuen WH, Fu J, Huang G, Melendez AJ, Ibrahim FB, Lu H, Cao X. The mitochondrial respiratory chain controls intracellular calcium signaling and NFAT activity essential for heart formation in *Xenopus laevis*. Mol Cell Biol 2007;27:6420–32.
Cobaleda C, Pérez-Caro M, Vicente-Dueñas C, Sánchez-García I. Function of the zinc-finger transcription factor SNAI2 in cancer and development. Annu Rev Genet 2007;41:41–61.
Deng ZL, Sharff KA, Tang N, Song WX, Luo J, Luo X, Chen J, Bennett E, Reid R, Manning D, Xue A, Montag AG, Luu HH, Haydon RC, He TC. Regulation of osteogenic differentiation during skeletal development. Front Biosci 2008;13:2001–21.
Folmes CD, Dzeja PP, Nelson TJ, Terzic A. Mitochondria in control of cell fate. Circ Res 2012;110:526–9.
Fromigue O, Hay E, Barbara A, Marie PJ. Essential role of nuclear factor of activated T cells (NFAT)-mediated Wnt signaling in osteoblast differentiation induced by strontium ranelate. J Biol Chem 2010;285:25251–8.

Gardin C, Vindigni V, Bressan E, Ferroni L, Nalesso E, Puppa AD, D'Avella D, Lops D, Pinton P, Zavan B. Hyaluronan and fibrin biomaterial as scaffolds for neuronal differentiation of adult stem cells derived from adipose tissue and skin. Int J Mol Sci 2011;12:6749–64.

Goettsch C, Rauner M, Hamann C, Sinningen K, Hempel U, Bornstein SR, Hofbauer LC. Nuclear factor of activated T cells mediates oxidised LDL-induced calcification of vascular smooth muscle cells. Diabetologia 2011;54:2690–701.

Hock MB, Kralli A. Transcriptional control of mitochondrial biogenesis and function. Annu Rev Physiol 2009;71:177–203.

Hogan PG, Chen L, Nardone J, Rao A. Transcriptional regulation by calcium, calcineurin, and NFAT. Genes Dev 2003;17:2205–32.

Horsley V, Pavlath GK. NFAT: ubiquitous regulator of cell differentiation and adaptation. J Cell Biol 2002;156:771–4.

Kim CH, Jeon HM, Lee SY, Ju MK, Moon JY, Park HG, Yoo MA, Choi BT, Yook JI, Lim SC, Han SI, Kang HS. Implication of snail in metabolic stress-induced necrosis. PLoS ONE 2011;6:e18000.

Kim MS, Usachev YM. Mitochondrial Ca^{2+} cycling facilitates activation of the transcription factor NFAT in sensory neurons. J Neurosci 2009;29:12101–14.

Koga T, Matsui Y, Asagiri M, Kodama T, de Crombrugghe B, Nakashima K, Takayanagi H. NFAT and Osterix cooperatively regulate bone formation. Nat Med 2005;11:880–5.

Kuznetsov AV, Margreiter R. Heterogeneity of mitochondria and mitochondrial function within cells as another level of mitochondrial complexity. Int J Mol Sci 2009;10:1911–29.

Lambertini E, Lisignoli G, Torreggiani E, Manferdini C, Gabusi E, Franceschetti T, Penolazzi L, Gambari R, Facchini A, Piva R. Slug gene expression supports human osteoblast maturation. Cell Mol Life Sci 2009;66:3641–53.

Leigh-Brown S, Enriquez JA, Odom DT. Nuclear transcription factors in mammalian mitochondria. Genome Biol 2010;11:215.

Madeira VM. Overview of mitochondrial bioenergetics. Methods Mol Biol 2012;810:1–6.

Mandal S, Lindgren AG, Srivastava AS, Clark AT, Banerjee U. Mitochondrial function controls proliferation and early differentiation potential of embryonic stem cells. Stem Cells 2011;29:486–95.

Marinov GK, Wang YE, Chan D, Wold BJ. Evidence for site-specific occupancy of the mitochondrial genome by nuclear transcription factors. PLOS ONE 2014;9:e84713.

Ogasawara T, Ohba S, Yano F, Kawaguchi H, Chung UI, Saito T, Yonehara Y, Nakatsuka T, Mori Y, Takato T, Hoshi K. Nanog promotes osteogenic differentiation of the mouse mesenchymal cell line C3H10T1/2 by modulating bone morphogenetic protein (BMP) signaling. J Cell Physiol 2013;228:163–71.

Parker GC, Acsadi G, Brenner CA. Mitochondria: determinants of stem cell fate? Stem Cells Dev 2009;18:803–6.

Penolazzi L, Lisignoli G, Lambertini E, Torreggiani E, Manferdini C, Lolli A, Vecchiatini R, Ciardo F, Gabusi E, Facchini A, Gambari R, Piva R. Transcription factor decoy against NFATc1 in human primary osteoblasts. Int J Mol Med 2011;28:199–206.

Pietilä M, Lehtonen S, Närhi M, Hassinen IE, Leskelä HV, Aranko K, Nordström K, Vepsäläinen A, Lehenkari P. Mitochondrial function determines the viability and osteogenic potency of human mesenchymal stem cells. Tissue Eng Part C: Methods 2010;16:435–45.

Shibanuma M, Ishikawa F, Kobayashi M, Katayama K, Miyoshi H, Wakamatsu M, Mori K, Nose K. Critical roles of the cAMP-responsive element-binding protein-mediated pathway in disorganized epithelial phenotypes caused by mitochondrial dysfunction. Cancer Sci 2012;103:1803–10.

Shutt TE, Bestwick M, Shadel GS. The core human mitochondrial transcription initiation complex: it only takes two to tango. Transcription 2011;2:55–9.

Stern PH. The calcineurin–NFAT pathway and bone: intriguing new findings. Mol Interv 2006;6:193–6.

Szczepanek K, Lesnefsky EJ, Larner AC. Multi-tasking: nuclear transcription factors with novel roles in the mitochondria. Trends Cell Biol 2012;22:429–37.

Torreggiani E, Lisignoli G, Manferdini C, Lambertini E, Penolazzi L, Vecchiatini R, Gabusi E, Chieco P, Facchini A, Gambari R, Piva R. Role of Slug transcription factor in human mesenchymal stem cells. J Cell Mol Med 2012;16:740–51.

Wanet A, Remacle N, Najar M, Sokal E, Arnould T, Najimi M, Renard P. Mitochondrial remodelling in hepatic differentiation and dedifferentiation. Int J Biochem Cell Biol 2014;54:174–85.

Wu WS, Heinrichs S, Xu D, Garrison SP, Zambetti GP, Adams JM, Look AT. Slug antagonizes p53-mediated apoptosis of hematopoietic progenitors by repressing puma. Cell 2005;123:641–53.

Yeo H, Beck LH, Thompson SR, Farach-Carson MC, McDonald JM, Clemens TL, Zayzafoon M. Conditional disruption of calcineurin B1 in osteoblasts increases bone formation and reduces bone resorption. J Biol Chem 2007;282:35318–27.

Zanotti S, Smerdel-Ramoya A, Canalis E. Reciprocal regulation of Notch and nuclear factor of activated T-cells (NFAT) c1 transactivation in osteoblasts. J Biol Chem 2011;286:4576–88.